

Delay time and tunneling transient phenomena

Gastón García-Calderón^{1,*} and Jorge Villavicencio^{1,2†}

¹*Instituto de Física, Universidad Nacional Autónoma de México, Apartado Postal 20 364, 01000 México, Distrito Federal, Mexico*

²*Facultad de Ciencias, Universidad Autónoma de Baja California, Apartado Postal 1880, 22800 Ensenada, Baja California, Mexico*

(Received 6 May 2002; revised manuscript received 26 June 2002; published 16 September 2002)

Analytic solutions to the time-dependent Schrödinger equation for cutoff wave initial conditions are used to investigate the time evolution of the transmitted probability density for tunneling. For a broad range of values of the potential barrier opacity α , we find that the probability density exhibits two evolving structures. One refers to the propagation of a *forerunner* related to a *time domain resonance* [Phys. Rev. A **64**, 0121907 (2001)], while the other consists of a semiclassical propagating wave front. We find a regime where the *forerunners* are absent, corresponding to positive *time delays*, and show that this regime is characterized by opacities $\alpha < \alpha_c$. The critical opacity α_c is derived from the analytical expression for the *delay time*, which reflects a link between transient effects in tunneling and the *delay time*.

DOI: 10.1103/PhysRevA.66.032104

PACS number(s): 03.65.Xp, 03.65.Ca, 73.40.Gk

I. INTRODUCTION

In recent times there have been relevant technological advances that have made it possible to design and construct artificial quantum structures at nanometric scales [1,2]. On the theoretical side, the above achievements have stimulated work on the issue of time-dependent tunneling. In particular, one finds a number of works that deal with the solution to the time-dependent Schrödinger's equation for cutoff wave initial states [3–6]. One interesting feature of these approaches is that at asymptotically long times the time-dependent solution goes into the well-known stationary solution. This establishes a bridge between time-dependent and time-independent approaches that may be used to address some subtle questions, such as the controversial problem of the relevant time scales for tunneling [7].

In a recent work we have used a time-dependent analytic solution to the Schrödinger equation for an arbitrary potential [5], to explore the tunneling dynamics for a rectangular potential barrier [6]. We found that the probability density exhibits a transient structure that we named *time domain resonance*, and obtained that it provides the largest probability of finding the tunneling particle at the potential barrier edge. Moreover, we discussed the relevant time scales associated with the *time domain resonance* as a function of the potential parameters and the incidence energy.

The purpose of this work is to extend the above investigation to study the time evolution of the probability density along the transmitted region of the potential. We found that for a large variation of potential parameters, the probability density exhibits two evolving structures. One of them is a *forerunner* that corresponds to the time propagation of the *time domain resonance*, whereas the other structure consists of a propagating wave front. We find that the *forerunner* vanishes at asymptotically long times and distances from the interaction region, whereas the propagating wave front tends to the stationary solution of the problem. The propagating

wave front exhibits a time delay with respect to the free case situation. We corroborate that this dynamical *delay time* is accurately described by the analytical expression obtained from the phase energy derivative of the transmission amplitude. The analysis of this time scale as a function of the potential parameters yields positive and negative (time-advance) *delay times*. We have found that *forerunners* exist whenever the *delay time* is negative, thus establishing a deep connection between transient and asymptotic effects in tunneling.

The paper is organized as follows. Section II provides the main expressions of the formalism, which are relevant to calculate the probability density along the transmitted region. In Sec. III we consider the time honored rectangular barrier potential model. Here we study through several subsections the time evolution of the transmitted probability density, and discuss the *delay time*. Finally, in Sec. IV we present the conclusions.

II. FORMALISM

The relevant expressions to calculate the time evolution of the transmitted wave with the reflecting cutoff wave initial condition were considered in Ref. [6]. They follow from a general formalism developed by García-Calderón [5] for the solution of the time-dependent Schrödinger equation for tunneling through an arbitrary potential $V(x)$ that vanishes outside a region $0 \leq x \leq L$. Our approach is a generalization of the free case problem considered by Moshinsky [8] that led to the *diffraction in time* phenomenon. This transient effect has been recently verified experimentally [9] and has stimulated further studies [10].

For the sake of completeness and to fix the notation we recall the relevant equations here. The cutoff wave initial condition corresponding to a reflecting wave may be written as

$$\psi(x, k; t=0) = \begin{cases} e^{ikx} - e^{-ikx}, & x \leq 0 \\ 0, & x > 0. \end{cases} \quad (1)$$

*Electronic address: gaston@fisica.unam.mx

†Electronic address: villavics@uabc.mx

The time-dependent solution $\psi(x, k; t)$ of Schrödinger's equation for the transmitted region, $x \geq L$ reads,

$$\psi(x, k; t) = \psi_q(x, k; t) + \psi_r(x, k; t), \quad (2)$$

where ψ_q is given by

$$\psi_q(x, k; t) = T_k M(y_k) - T_{-k} M(y_{-k}) \quad (3)$$

and ψ_r by

$$\psi_r(x, k; t) = - \sum_n^{\infty} T_n M(y_{k_n}). \quad (4)$$

In the above expressions the quantities T_k and $T_{-k} = T_k^*$ refer, respectively, to transmission amplitudes and $T_n = 2ik u_n(0) u_n(L) \exp(-ik_n L) / (k^2 - k_n^2)$ is given in terms of the set of resonant states $\{u_n(x)\}$ and the complex poles $\{k_n = a_n - ib_n\}$ of the problem [5]. The functions $M(y_s)$ are defined as [5]

$$M(y_s) = \frac{1}{2} e^{(imx^2/2\hbar t)} w(iy_s), \quad (5)$$

where the $w(iy_s)$ is the complex error function [12] with the argument y_s given by

$$y_s \equiv e^{-i\pi/4} \left(\frac{m}{2\hbar t} \right)^{1/2} \left[x - \frac{\hbar s}{m} t \right]. \quad (6)$$

In Eqs. (5) and (6), s stands for either $\pm k$ or $k_{\pm n}$, and the index n refers to a given complex pole. Poles are located on the third and fourth quadrants of the complex k plane. The free case solution to the above problem for a cutoff plane wave was considered by Moshinsky [8]. The solution for the free case with a reflecting initial condition is given by

$$\psi_0(x, k; t) = M(y_k) - M(y_{-k}). \quad (7)$$

Note that in the absence of a potential, i.e., $T_k = 1$, the term ψ_q , given by Eq. (3), becomes identical to the free case solution ψ_0 given above. We shall refer to ψ_q , which resembles the free contribution, as the *quasimonochromatic contribution* and to the sum term given by Eq. (4), namely, ψ_r , as the *resonant contribution*. From the analysis given in Ref. [5] one can see that the exact solution $\psi = \psi_q + \psi_r$, given by Eq. (2), satisfies the initial condition and that at asymptotic long times, $\psi_r \rightarrow 0$ and ψ_q goes into the stationary solution. Hence at very long times ψ becomes

$$\psi(x, k; t) = T_k e^{ikx} e^{-iEt/\hbar}. \quad (8)$$

As pointed out in Ref. [6] a cutoff wave initial state has, in addition to tunneling components, momentum components that go above the barrier height. One sees from Eq. (2), that the probability density exhibits and interplay between tunneling and over-the-barrier processes. However, as Eq. (8) indicates, at asymptotically long times, the transient effects vanish and one ends up with a stationary tunneling solution.

III. THE MODEL

As has been customary in studies involving tunneling times in one dimension, we consider a model that has been used extensively in studies on time-dependent tunneling, namely, the rectangular barrier potential, characterized by a height V_0 in the region $0 \leq x \leq L$. To calculate the time-dependent solution $\psi(x, k; t)$ given by Eq. (2), in addition to the barrier parameters V_0 , L , and the corresponding incidence energy $E = \hbar^2 k^2 / 2m$, we need to determine the complex poles $\{k_n\}$ and the resonant states $\{u_n(x)\}$ of the system. Both the complex poles $\{k_n\}$ and the corresponding resonant eigenfunctions $\{u_n(x)\}$ can be calculated using a well established method, as discussed elsewhere [5,6]. For the rectangular potential barrier the set of complex energies $E_n = \hbar^2 k_n^2 / 2m = \varepsilon_n - i\Gamma_n / 2$ corresponds to the poles of the transmission amplitude of the problem [6], and hence it may be used to describe the well-known top-barrier transmission resonances appearing in that system.

A. Dynamics of the transmitted probability density

To exemplify the time evolution of the probability density in the transmitted region we consider a set of parameters typical of semiconductor artificial quantum structures [1]: $V_0 = 0.3$ eV, $L = 5.0$ nm, $E = 0.01$ eV, and $m = 0.067 m_e$, with m_e the electron mass. Our choice of parameters is the same as in Ref. [6], and it guarantees that most momentum components of the initial state tunnel through the potential. The different parameters may also be expressed in terms of the opacity α defined as

$$\alpha = k_0 L, \quad (9)$$

where $k_0 = [2mV_0]^{1/2} / \hbar$, and the ratio $u = V_0 / E$. In our case $\alpha = 3.63$ and $u = 30$. For example, the regime of opaque barrier is reached for values of $\alpha > 5$. In what follows we shall explore the time evolution of $|\psi|^2$ at several positions x_0 away from the interaction region. From Eq. (2) we can write

$$|\psi|^2 = |\psi_q|^2 + |\psi_r|^2 + I_{rq}, \quad (10)$$

where $I_{rq} = 2\text{Re}(\psi_q^* \psi_r)$ stands for the corresponding interference term. Figure 1 displays the time evolution of $|\psi|^2$ (solid line) at the right edge of the potential barrier, $x = L$, as considered in Ref. [6]. This is the same example exhibited in Fig. 2 of Ref. [6] using a larger time scale. The sharp peak at very short times is mainly due to the resonant contribution $|\psi_r|^2$ (dotted line). As discussed in Ref. [6], the maximum value of this *time domain resonance*, t_p , provides a tunneling time scale representing the largest probability to find the particle at the barrier edge. In our example $t_p = 5.4$ fs. The figure also shows the quasimonochromatic contribution $|\psi_q|^2$ (dashed line) that rises and oscillates with time in a manner resembling the free case $|\psi_0|^2$ (dashed-dotted line). The interference contribution I_{rq} is not shown, although clearly it is necessary to account for the complete solution.

Along the transmitted region, $x > L$, the probability density becomes a propagating solution. We can see that the *time domain resonance* becomes a propagating structure that we

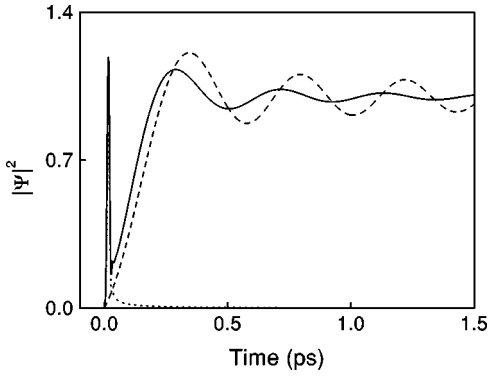


FIG. 1. Time evolution of the normalized probability density $|\psi|^2$ (solid line) at the barrier edge $x=L$. The main contribution to the *time domain resonance* comes from the resonant term $|\psi_r|^2$ (dotted line), the quasimonochromatic contribution $|\psi_q|^2$ (dashed line) oscillates with time in a similar fashion as the free solution $|\psi_0|^2$ [8] (dashed-dotted line). The system parameters are: $V_0 = 0.3$ eV, $L = 5.0$ nm, and $E = 0.01$ eV, see text.

shall refer to as *forerunner*. Figure 2 shows the case for $x_0 = 50.0$ nm. One sees that the amplitude of this transient structure (dotted line) is smaller than the quasimonochromatic contribution (dashed line). Note also that the solution has separated itself into two well defined structures that propagate with different velocities. The *forerunner* propagates with a velocity given approximately by $v_r = \hbar a_1 / m$, the velocity associated with the first top-barrier resonance, whereas the quasimonochromatic contribution does that, approximately by $v_k = \hbar k / m$, the velocity associated with the incident particle. From a physical point of view we can understand the above situation by noting that our initial state possesses momentum components in k space above the barrier, which can be transmitted more effectively by the resonance window corresponding to the first top-barrier resonance. This is the origin of the fast tunneling response, given by the *forerunner*, mainly described by $|\psi_r|^2$. In our example, the main contribution to the resonant term, $|\psi_r|^2$, comes from the first top-barrier resonant state. However, depending on the distance x_0 , one may need to sum up over many terms to account for the complete wave function. The

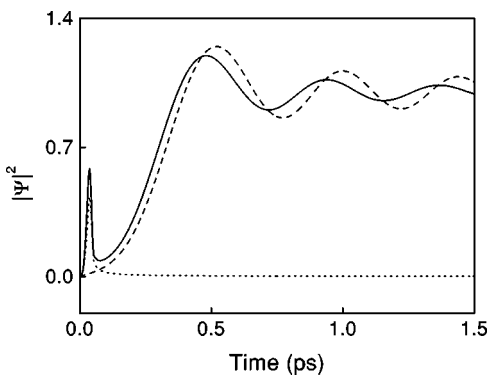


FIG. 2. Time evolution of $|\psi|^2$ (solid line) at the fixed position $x_0 = 50.0$ nm. $|\psi_r|^2$ (dotted line) and $|\psi_q|^2$ (dashed line) account, respectively, for the *forerunner* and the quasimonochromatic contributions, see text.

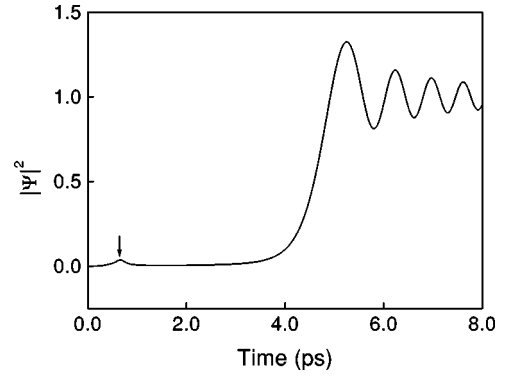


FIG. 3. Time evolution of $|\psi|^2$ at the fixed position $x_0 = 1000.0$ nm. Notice that the *forerunner* has almost disappeared (an arrow indicates its position). The parameters are the same as in Fig. 1.

second type of response is given in a natural way by the maximum of the first peak of the probability density associated with the quasimonochromatic contribution $|\psi_q|^2$. This comes mostly from the momentum components centered about the momentum $\hbar k$, which tunnel through the structure.

At still much larger distances, $x_0 = 1000.0$ nm as shown in Fig. 3, the *forerunner* has disappeared almost completely, and the time evolution of the probability density is dominated by $|\psi_q|^2$.

The behavior of the *forerunner* may be understood qualitatively by using the asymptotic properties [5] of the $M(y_{k_{\pm n}})$ functions in Eq. (4). By numerical inspection we find that at a fixed position x_0 , the main features of the *forerunner* can be described using the one-term ($n=1$) approximation to Eq. (4), namely, $|\psi_f|^2 = |T_1 M(y_{k_1})|^2$. Since in the vicinity of the peak of the *forerunner* the argument y_{k_1} of $M(y_{k_1})$ lies within $-\pi/2 < \arg y_{k_1} < \pi/2$, one obtains $|\psi_f|^2 = (4\pi)^{-1} |T_1 / y_{k_1}|^2$. This allows us to write a simple analytical expression for the time evolution of this transient structure, namely,

$$\frac{|\psi_f|^2}{|T_1|^2} = \frac{1}{2\pi} \frac{(\hbar t/m)}{[(x_0 - \hbar a_1 t/m)^2 + (\hbar b_1 t/m)^2]}. \quad (11)$$

From the above equation we can see that the peak of the *forerunner* propagates with a velocity $v_r = \hbar a_1 / m$, as discussed earlier in the text. Figure 4 exhibits a plot of $|\psi_f|^2$ (dashed line) as a function of time for the same parameters used in Fig. 1. We observe good agreement with the exact calculation of $|\psi|^2$ (solid line), given by Eq. (2). It is worthwhile to point out by inspection of Eq. (11) that as time increases, the maximum of the *forerunner*, occurring at $\tau = x_0 / v_r$, diminishes at a rate proportional to x_0^{-1} . Hence, for an increasing value of x_0 , the transient structure tends to a vanishing value.

It is interesting to mention that in the case of opaque barriers, i.e., $\alpha > 5.0$, the resonant contribution $|\psi_r|^2$ may be much larger than the quasimonochromatic contribution $|\psi_q|^2$. This occurs even at quite large distances from the

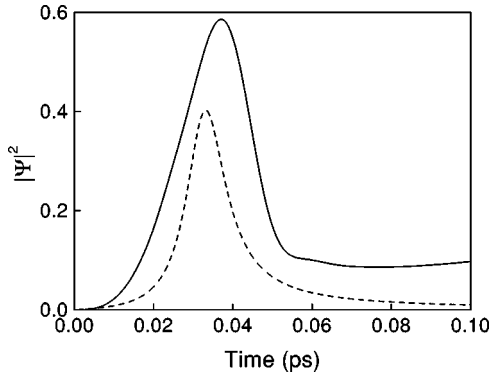


FIG. 4. Comparison between the formula for the forerunner, $|\psi_f|^2$ (dashed line), and the exact solution, $|\psi|^2$ (solid line), as a function of time for a fixed value of the position $x_0=50.0$ nm. The parameters are the same as in Fig. 1.

interaction region. Figure 5 exhibits an example of this situation for $L=15.0$ nm and a distance $x_0=1 \times 10^5$ nm from the potential. Since the solution is normalized to $|T_k|^2$ and this quantity becomes very small for large L , one sees that $|\psi_r|^2$ is several orders of magnitude larger than $|\psi_q|^2$, depicted in the inset of that figure. Clearly, as previously discussed, and exemplified in Fig. 3, at still much larger values of the distance x_0 , the term $|\psi_q|^2$ shall eventually dominate over $|\psi_r|^2$.

Let us now discuss another interesting behavior of the forerunner. In Fig. 6 we plot it as a function of time at a given distance $x_0 > L$, for different values of the barrier thickness, $L=5.0$ nm (solid line), $L=4.5$ nm (dashed line), $L=3.0$ nm (dotted line), and $L=2.0$ nm (dashed-dotted line), for the same parameters used in Fig. 1. We can see that the intensity of the transient structure diminishes as L decreases. In fact, for the case of a barrier width $L=2.0$ nm, we observe that the forerunner disappears. However, as shown in the inset of Fig. 6, what happens is that both the resonant contribution, $|\Psi_r|^2$, and the interference term, I_{rq} , in Eq. (10) for the probability density, are not only overwhelmed by the monochromatic contribution $|\Psi_q|^2$ but also almost cancel each other.

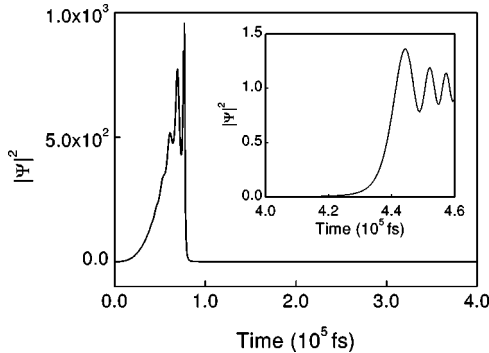


FIG. 5. The main graph shows the time evolution of $|\psi|^2$ for the case of an opaque barrier of width $L=15.0$ nm ($\alpha=10.88$), at a fixed position $x_0=1 \times 10^5$ nm. Notice that the forerunner, given essentially by the resonant contribution $|\psi_r|^2$, overwhelms the quasimonochromatic term described by $|\psi_q|^2$, as depicted in the inset, see text.

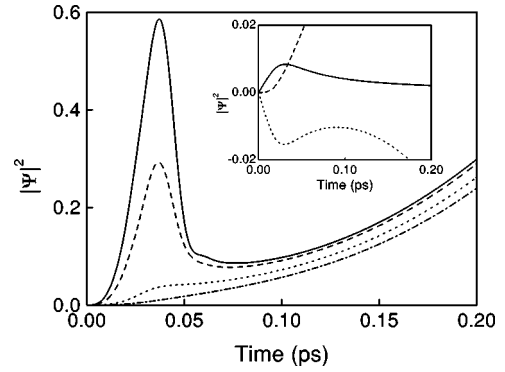


FIG. 6. Time evolution of the forerunner for a fixed value of the position $x_0=50.0$ nm, for different values of the barrier width L : (a) 5.0 nm (solid line), (b) 4.5 nm (dashed line), (c) 3.0 nm (dotted line), and (d) 2.0 nm (dashed-dotted line). Notice that the transient structure disappears as the barrier width diminishes. The parameters are the same as in Fig. 1. The inset exhibits a plot of the contributions to $|\Psi|^2$ (dashed line) of case (d). Notice that the resonant contribution $|\Psi_r|^2$ (solid line) that gives rise to the forerunner, is almost canceled out entirely by the interference contribution I_{rq} (dotted line).

Similarly Fig. 7 shows that the forerunner also disappears by diminishing the barrier height V_0 , and again, as the inset shows, this occurs by the same reason as discussed in the previous case. The above results hold also for the time domain resonance, i.e., at $x=L$. From the above analysis one could argue that the existence of the time domain resonance, and hence of the forerunners, depends basically on a particular combination of the parameters V_0 and L . In the following subsection we shall show that this is indeed the case.

B. Delay time and forerunners

An interesting result of the analysis of the preceding subsection, depicted by Fig. 3, is that at very large distances

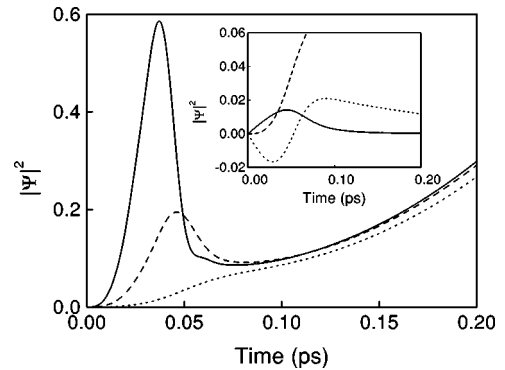


FIG. 7. Time evolution of the forerunner for a fixed value of the position $x_0=50.0$ nm, for three different values of the barrier potential V_0 : (a) 0.3 eV (solid line), (b) 0.2 eV (dashed line), and (c) 0.1 eV (dotted line). Notice that the amplitude of the forerunner decreases as the barrier height of the potential diminishes. At the inset we plot the contributions to $|\Psi|^2$ (dashed line) of case (c). Notice that the resonant contribution $|\Psi_r|^2$ (solid line) is almost canceled out by the interference contribution I_{rq} (dotted line). The parameters are the same as in Fig. 1.

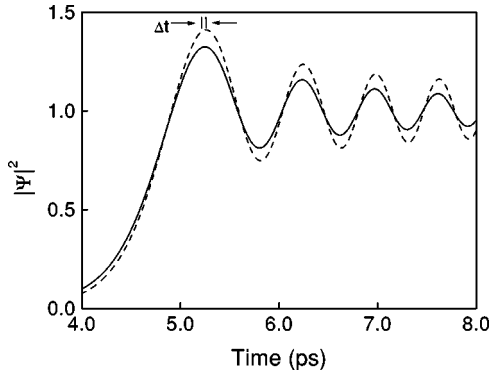


FIG. 8. Time advance of the solution $|\psi|^2$ (solid line) relative to the free propagation case, $|\psi_0|^2$ (dashed line). The parameters are the same as in Fig. 1.

from the interaction region the time evolution of the probability density $|\psi|^2$ is essentially given by $|\psi_q|^2$ and exhibits a well-defined wave front. As mentioned above, the wave front propagates with approximately the classical velocity $v_k = (\hbar k/m)$, as follows by direct inspection of the argument to the M function, given by Eq. (6). A comparison of $|\psi|^2$ near the above wave front with the corresponding free probability density $|\psi_0|^2$ is exhibited in Fig. 8. The parameters and the value of the position x_0 are the same as in Fig. 3. Both solutions look very much alike. Note that its corresponding wave fronts are slightly displaced with respect to each other. In fact the maximum values of $|\psi|^2$ and $|\psi_0|^2$, for the parameters used in our example, exhibit a time difference that corresponds to a negative *delay time* (time advance).

The above considerations lead us to the notion of *delay time* as discussed by Bohm [13]. He has argued that the main contribution to the transmitted probability density comes from values in the neighborhood of space, for which the phase of the wave function changes slowly with energy. This yields the well-known expression for the *delay time* [13] as $t_\phi = (d\phi/dk)/v_k$, where ϕ stands for the phase of the transmission amplitude, i.e., $T_k = |T_k| \exp(i\phi)$ and v_k is the classical velocity as defined above. For the case of the rectangular potential barrier the *delay time* reads

$$t_\phi = \frac{m}{\hbar k \kappa} \left[\frac{k_0^4 \sinh(2\kappa L) - 2\kappa L k^2 (k^2 - \kappa^2)}{4k^2 \kappa^2 + k_0^4 \sinh^2(\kappa L)} \right] - \frac{mL}{\hbar k}. \quad (12)$$

We define Δt as the time difference of the maximum values of the curves for $|\psi|^2$ and $|\psi_0|^2$ obtained numerically, namely,

$$\Delta t = |\psi^{max}|^2 - |\psi_0^{max}|^2. \quad (13)$$

Figure 9 displays a plot of Δt (full squares) and the *delay time* t_ϕ (solid line), as a function of the barrier width L for a large fixed value of the position x_0 . One sees that Δt reproduces exactly the behavior obtained from the analytical expression for t_ϕ . The above agreement of Δt with t_ϕ does not hold when the distance x_0 is very close to the interaction region. There, the effect of the transient structure cannot be

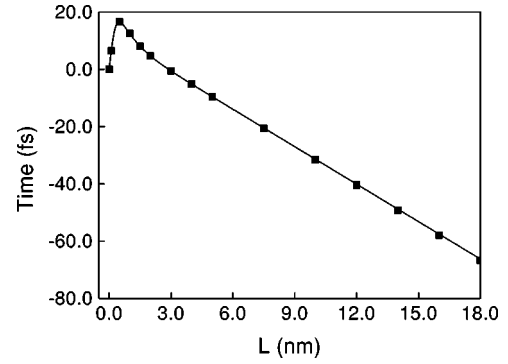


FIG. 9. Plot of Δt (full squares) and the *delay time* t_ϕ (solid line) as a function of the barrier width L , at fixed position $x_0 = 1 \times 10^5$ nm, with the same parameters as in Fig. 1. Here $k_0 = 0.07258$ and hence α varies from 7.25×10^{-3} to 13.065, see text.

ignored. Figure 1 exhibits this situation for $x_0 = L$. The behavior of $|\psi|^2$ (solid line) is very different from that of the free contribution $|\psi_0|^2$ (dashed-dotted line). As discussed previously, the *time domain resonance* peak comes from the resonant contribution. The splitting of the solution observed at larger distances and longer times has yet not occurred.

Note also in Fig. 9 that for thin barriers there is a positive *delay time*, and as L increases, there is a transition to a negative *delay time*. In what follows we shall demonstrate that such a transition occurs for a critical value of the opacity α_c . In order to show the latter, let us rewrite Eq. (12) as a function of the parameters α and $u = V_0/E$, namely,

$$\frac{t_\phi}{t_0} = \frac{[4\gamma^{-1} \sinh \gamma - \cosh \gamma + \gamma^2 \alpha^{-2} - 3]}{[\gamma^2 \alpha^{-2} - \gamma^4 \alpha^{-4}/4 + \sinh^2(\gamma/2)][4 - \gamma^2 \alpha^{-2}]^{1/2}}, \quad (14)$$

where we have defined $t_0 = (mL/\hbar k_0)$ and $\gamma = 2\alpha(1 - u^{-1})^{1/2}$. Thus from Eq. (14) the condition for the transition from positive to negative *delay times*, i.e., $t_\phi = 0$, is simply given by the vanishing of the numerator, namely,

$$4\gamma^{-1} \sinh \gamma - \cosh \gamma = \left(3 - \frac{\gamma^2}{\alpha^2}\right). \quad (15)$$

For a particular value of the opacity α , we can determine from the above equation the value of u at which the transition occurs. However, one finds by inspection of Eq. (15) that such a transition is not possible for small values of α . That is, there exists a critical value of the opacity $\alpha = \alpha_c$ such that for $\alpha < \alpha_c$, the transition does not occur. This situation corresponds to impose the limit $u \rightarrow \infty$ in the solution to Eq. (15). This implies that $\gamma \rightarrow 2\alpha_c$, and hence Eq. (15) becomes

$$\cosh 2\alpha_c - 2\alpha_c^{-1} \sinh 2\alpha_c = 1. \quad (16)$$

The numerical solution to Eq. (16) yields the critical opacity $\alpha_c = 2.0653$. Note that in addition to the potential parameters V_0 and L , the opacity depends on the mass m of the incident particle. It turns out that this value of α_c accounts for sys-

tems where the potential barrier is either too shallow or too thin. Therefore, in the regime $\alpha < \alpha_c$, only a positive *delay time* is observed.

We have also found that α_c plays an important role in the existence of *time domain resonances* and hence of *forerunners*. In fact, we find that for systems where $\alpha < \alpha_c$, no *time domain resonances* nor *forerunners* are observed. This behavior can be seen in Figs. 6 and 7. For example, in the cases (c) and (d) of Fig. 6, which correspond to barrier widths $L = 3.0$ nm and $L = 2.0$ nm, the parameter α is, respectively, 2.17 and 1.45. Clearly in case (d) the forerunner has completely disappeared. In Fig. 7, the cases (b) and (c) corresponding to the potential heights $V_0 = 0.2$ eV and $V_0 = 0.1$ eV, which refer, respectively, to the values of α , 2.96 and 2.095. In this case the disappearance of the *forerunner* occurs in the vicinity of the critical opacity α_c .

C. Comment on the phase-delay time

Hartman has argued [11] that the time it takes for a particle to traverse the classical forbidden region of a potential barrier can be obtained from an analysis involving the *delay time*. He referred to this quantity as the *transmission time* τ_H , though nowadays it is often called *phase-delay time*. It corresponds to the difference between the time at which a transmitted particle of momentum $\hbar k$ would leave the rear of the barrier, $x=L$, and the time the same particle would arrive at the front of the barrier, $x=0$. The *transmission time* τ_H can be written as [see Eq. (13) of Ref. [11]],

$$\tau_H = t_\phi + t_0, \quad (17)$$

where t_ϕ is given by Eq. (12) and $t_0 = (mL/\hbar k)$ represents the free time across a distance equal to the barrier width L . Note that t_0 cancels out exactly the second term on the right-hand side of Eq. (17). The idea of considering τ_H as the relevant time scale for tunneling through a classically forbidden region has been criticized by arguing that there is no physical justification for relating in a causative sense the free evolving peak and the transmitted peak through a barrier [7,14]. Our analysis of the time evolution of the probability density supports this criticism. Indeed, as discussed in Sec. II A, along the transmitted region, the probability density may split into two structures evolving with different velocities. Hence it is not physically justified to choose a feature of one of them to compare it with the free evolving case. In particular, at the barrier edge $x=L$, for $\alpha > \alpha_c$, the behavior of probability density $|\psi(L,t)|^2$ is governed by the *time domain resonance*, which yields a completely different time scale [6] than the *phase-delay time*. Moreover, even for $\alpha < \alpha_c$, where there is no *time domain resonance*, our calculations do not support Hartman's transmission time τ_H . This is illustrated in Fig. 10(a), where we plot τ_H as a function of the barrier width L (solid line), and compare it with a plot of $\delta_H = \Delta t + t_0$ (full squares) measured dynamically at the barrier edge $x=L$. Although both curves exhibit a similar qualitative behavior, the values of τ_H and δ_H , are quite different. However, Figure 10(b) exhibits a plot of δ_H (full squares) as a function of the barrier width L , measured at a distance x_0

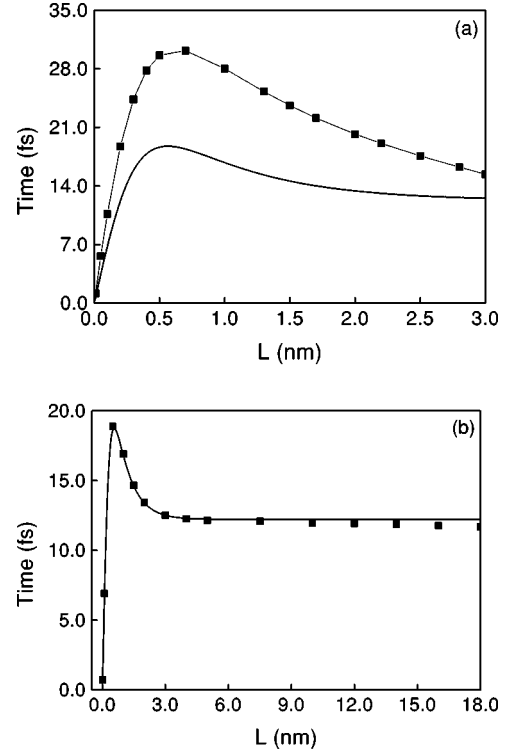


FIG. 10. Comparison of the *transmission time* τ_H (solid line) with δ_H (full squares) as a function of the barrier width L , measured at (a) the barrier edge $x=L$ and (b) at a fixed position $x_0 = 1 \times 10^5$ nm. The parameters are as in Fig. 1. Hence $k_0 = 0.7258$, and the opacity varies as mentioned in Fig. 9, see text.

very far away from the interaction region, i.e., $x_0 = 1.0 \times 10^5$ nm. This figure also shows a plot of τ_H (solid line) and we see that they match quite well for all values of α . The lack of agreement between the plots of τ_H and δ_H in Fig. 10(a) follows because the *time domain resonance*, the *quasi-monochromatic contribution*, and the *interference term* are very close together, as exemplified in Fig. 1 for $L = 5.0$ nm. However, at long distances the *forerunner* and the *quasi-monochromatic contribution* are quite separated, though it may be shown that the *interference term* accounts for the *delay time* [15].

In the opaque barrier regime, $\alpha \gg 1$, the above times become independent of the barrier width, giving rise to the well-known Hartman effect. Indeed at asymptotically large values of L , τ_H goes as $2m/(\hbar k \kappa)$ as follows by inspection of Eq. (17) [11]. As can be seen, it is only at long distances from the interaction region, when δ_H coincides with the dynamical time scale δ_H .

The above considerations, therefore, indicate that the *transmission time*, i.e., τ_H given by Eq. (17), does not represent the tunneling time of the particle through the classically forbidden region. The *phase time delay* t_ϕ , in the spirit of Wigner and Eisenbud [16], represents an asymptotic effect of the potential on the tunneling particle.

IV. CONCLUSION

Using an analytical solution to the time-dependent Schrödinger equation for cutoff semi-infinite initial waves, we

have investigated the dynamics of the transmitted probability density for tunneling through a rectangular potential barrier. We have found two regimes, characterized by a critical opacity parameter α_c , such that for values of $\alpha < \alpha_c$ there are no *domain resonances* and consequently no *forerunners*, whereas for $\alpha > \alpha_c$, these transient structures may exist depending on the value of $u = V_0/E$. The above result follows from an unexpected connection between the existence of these transient structures and the *delay time*. This deserves to be studied further. An interesting feature of the formalism used in this work is that it applies to arbitrary potential profiles of finite range. Hence, the existence of *forerunners*, for

a given problem, would depend on the interplay among the different contributions to the probability density given by Eq. (10). Our results suggest also that the study of transient effects cannot be ignored for a thorough understanding of the tunneling time problem.

ACKNOWLEDGMENTS

The authors acknowledge partial financial support of DGAPA-UNAM under Grant No. IN101301 and from Conacyt, México, through Contract No. 431100-5-32082E.

-
- [1] D. K. Ferry and S. M. Goodnick, *Transport in Nanostructures* (Cambridge University Press, Cambridge, UK, 1997), pp. 91–201.
- [2] H.C. Manoharan, C.P. Lutz, and D.M. Eigler, *Nature (London)* **403**, 512 (2000).
- [3] A.P. Jauho and M. Jonson, *Superlattices Microstruct.* **6**, 303 (1989).
- [4] S. Brouard and J.G. Muga, *Phys. Rev. A* **54**, 3055 (1996).
- [5] G. García-Calderón and A. Rubio, *Phys. Rev. A* **55**, 3361 (1997).
- [6] G. García-Calderón and J. Villavicencio, *Phys. Rev. A* **64**, 012107 (2001).
- [7] R. Landauer and Th. Martin, *Rev. Mod. Phys.* **66**, 217 (1994).
- [8] M. Moshinsky, *Phys. Rev.* **88**, 625 (1952).
- [9] P. Szriftgiser, D. Guéry-Odelin, M. Arndt, and J. Dalibard, *Phys. Rev. Lett.* **77**, 4 (1996); Th. Hils, J. Felber, R. Gähler, W. Gläser, R. Golub, K. Habichit, and P. Wille, *Phys. Rev. A* **58**, 4784 (1998).
- [10] Č. Brukner and A. Zeilinger, *Phys. Rev. A* **56**, 3804 (1997).
- [11] T.E. Hartman, *J. Appl. Phys.* **33**, 3427 (1962).
- [12] V. N. Faddeyeva and N. M. Terent'ev, *Mathematical Tables* (Pergamon, London, 1961); *Handbook of Mathematical Functions*, edited by M. Abramowitz and I. A. Stegun (Dover, New York, 1965), p. 297.
- [13] D. Bohm, *Quantum Theory* (Prentice-Hall, New York, 1951).
- [14] M. Büttiker and R. Landauer, *Phys. Rev. Lett.* **49**, 1739 (1982).
- [15] G. García-Calderón and A. Hernández (unpublished).
- [16] E.P. Wigner, *Phys. Rev.* **98**, 145 (1955); L. Eisenbud, Ph.D. thesis, Princeton University, 1948.